Tight Coupling of Surface and In-Plant Biochemistry and Convection Governs Key Fine Particulate Components over the Amazon Rainforest

Manish Shrivastava,* Quazi Z. Rasool, Bin Zhao, Mega Octaviani, Rahul A. Zaveri, Alla Zelenyuk, Brian Gaudet, Ying Liu, John E. Shilling, Johannes Schneider, Christiane Schulz, Martin Zöger, Scot T. Martin, Jianhuai Ye, Alex Guenther, Rodrigo F. Souza, Manfred Wendisch, and Ulrich Pöschl

ABSTRACT: Combining unique high altitude aircraft measurements and detailed regional model simulations, we show that in plant biochemistry plays a central but previously unidentified role in fine particulate forming processes and atmosphere−biosphere−climate interactions over the Amazon rainforest. Isoprene epoxydiol secondary organic aerosols (IEPOX SOA) are key components of sub micrometer aerosol particle mass throughout the troposphere over the Amazon rainforest and are traditionally thought to form by multiphase chemical pathways. Here, we show that these pathways are strongly inhibited by the solid thermodynamic phase state of aerosol particles and lack of particle and cloud liquid water in the upper troposphere. Strong diffusion limitations within organic aerosol coatings prevailing at low temperatures and low relative humidity in the upper troposphere strongly inhibit the reactive uptake of IEPOX to inorganic aerosols. We find that direct emissions of 2 methyltetrol gases formed by in plant biochemical oxidation and/or oxidation of deposited IEPOX gases on the surfaces of soils and leaves and their transport by cloud updrafts followed by their condensation at low temperatures could explain over 90% of the IEPOX SOA mass concentrations in the upper troposphere. Our simulations indicate that even near the surface, direct emissions of 2 methyltetrol gases represent a ubiquitous, but previously unaccounted for, source of IEPOX SOA. Our results provide compelling evidence for new pathways related to land surface−aerosol−cloud interactions that have not been considered previously.

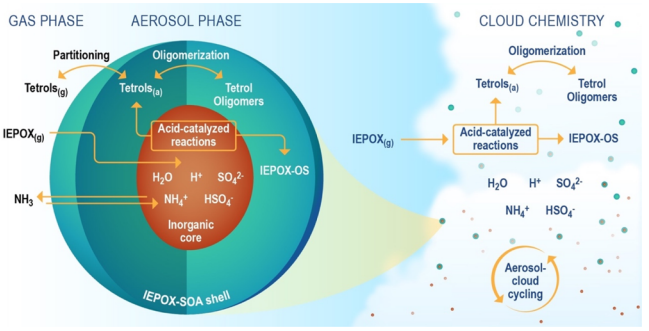

KEYWORDS: *secondary organic aerosol, plant biochemistry, surface chemistry, isoprene epoxydiols, Amazon rainforest, convection, fine particles*

INTRODUCTION

Isoprene is the most abundant nonmethane hydrocarbon emitted by vegetation with a global emission rate of ∼500 Tg y^{-1}, with a major contribution from the Amazon rainforest.[1] Isoprene is mainly thought to be oxidized in the atmosphere[2,3] but has also been reported to be oxidized within leaves.[4] Isoprene oxidation products significantly contribute to the formation of secondary organic aerosols (SOAs), particularly through multiphase chemical processes in aqueous aerosol particles and clouds.[5−9] Recent measurements of 2 methyltetrols over the Amazon proposed that direct emissions of 2 methyltetrols from the rainforest due to biological processes and environmental stressors were the most plausible explanation for their observations.[10] However, previous studies have largely focused on atmospheric chemical processes as a source of SOAs,[2,3] largely neglecting the potential role of in plant biochemical products in their formation.

One of the atmospheric SOA formation pathways, investigated most intensely in the last decade, is related to the reactive uptake of gas phase isoprene epoxydiols (IEPOX, formed by oxidation of isoprene) by aqueous inorganic sulfate particles to form SOAs (IEPOX SOA).[5,7] Within particles, IEPOX SOA formation is kinetically limited by diffusion in the viscous organic aerosol (OA) shell.[11] A recent experimental study shows that IEPOX SOA components of 2 methyltetrols and organosulfates are highly viscous and cause strong particle phase diffusion limitations as they form a coating around the inorganic seeds during their formation.[12]

Global modeling studies have found IEPOX SOA to be the major source of isoprene SOAs but often overestimate IEPOX SOA formation compared to measurements.[13−16] However, most of these modeling studies have not included the known effects of organic coatings and aerosol phase state on IEPOX SOA formation,[13,15,16] which could lead to large biases in predicted IEPOX SOA, especially in the upper troposphere.

Over the Amazon, key and unique aircraft measurements were collected using an aerosol mass spectrometer (AMS), which show that IEPOX SOA comprises ∼20% of the OA mass concentrations near the surface and in the upper troposphere on several days and over wide spatial extents.[17] Measurements over the Amazon rainforest also show that cloud updrafts could transport semivolatile organic gases to the upper troposphere where they condense to form increasing particle numbers[18] and mass concentrations.[19]

Here, we conduct detailed regional model simulations over the Amazon to show that IEPOX SOA formation in the upper troposphere cannot be explained by traditional atmospheric chemistry, reflecting a large gap in our understanding of IEPOX SOA processes in the upper troposphere. Our results contrast previous global modeling studies, which reported overprediction of IEPOX SOA,[13,15,16] likely because those studies neglected the role of particle phase diffusion limitations as described above.

We include the recently discovered estimates of plant biochemical emissions of semivolatile 2 methyltetrol gases[10] within a detailed regional model and show that their convective transport to the upper troposphere and their subsequent condensation due to cold upper troposphere temperatures (∼225 K) are the most plausible explanations, which close the large gap between model predictions and aircraft observations,[17] and this plant source far exceeds IEPOX SOA formation through atmospheric chemistry in the upper troposphere. We find that this plant source contributes significantly to IEPOX SOA even near the surface. A previous study conducted direct chiral measurements over the Amazon and indicated that more than 69% of the 2 methyltetrols found in particles with diameters less than 10 μm originated from primary biological sources.[20] Our results show that methyltetrols in the submicron range (<1 particle μm) as well likely originate from biological sources as gases. These gases then condense to particle phase methyltetrols.

METHODS

Safety statement: no unexpected or unusually high safety hazards were encountered.

HALO Aircraft-Based Observational Estimates of IEPOX-SOA. Measurements of IEPOX SOA were made onboard the HALO aircraft both near the surface and the upper troposphere using an AMS. High altitude measurements of IEPOX SOA are especially unique and are used to evaluate WRF Chem predictions at near surface (0−2 km altitude) and upper troposphere (10−14 km) altitudes. Figure S1 shows the locations of the HALO aircraft flight transects. Detailed descriptions of IEPOX SOA observational estimates using the AMS mounted onboard the HALO aircraft were provided in Schulz et al.[17] and are briefly described in the Supporting Information, *HALO aircraft based observational estimates of IEPOX SOA*. AMS data measured onboard the HALO below 2 km altitude were corrected for inlet transmission effects according to the in situ comparison between the HALO and G1 as reported in Mei et al.[21] The uncertainty of IEPOX SOA estimated by this approach is lower at high altitudes (where biogenic SOA dominates), compared to lower altitudes where biomass burning also contributes significantly to OA (Figures 1d and S2), with an overall estimated uncertainty within a factor of 2.[8]

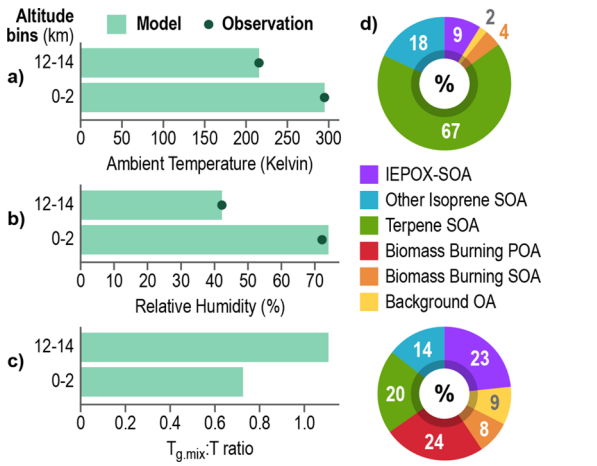

Figure 1. HALO aircraft measured and WRF Chem simulated averaged quantities on September 21, 2014, near the surface (0−2 km altitude) and the upper troposphere (12−14 km altitude): (a) ambient temperature, (b) ambient RH (%), (c) simulated ratio of the glass transition temperature of OA to ambient temperature ($T_{g,mix}/T$), and (d) simulated composition of OA. Black dots in (a,b) represent measurements, while horizontal bars are model predictions. Pie charts in (d) indicate that monoterpene SOA dominates upper tropospheric OA (top pie chart), representing highly viscous SOA coatings, while near the surface (bottom pie chart), no single SOA component is dominant.

IEPOX-SOA Formation. The detailed mechanisms and equations governing the multiphase reactive uptake of IEPOX and the role of viscous SOA coatings limiting IEPOX SOA formation, which we implemented in WRF Chem, are described in the Supporting Information, *IEPOX reactive uptake*, and Tables S1 and S2. This mechanism was also recently evaluated against laboratory single particle measurements of IEPOX SOA formation in a Teflon chamber at timescales of ∼hours under low relative humidity (RH) conditions.[22] Figure 2 schematically illustrates simulated multiphase chemistry processes occurring during the reactive uptake of IEPOX gas on aqueous inorganic aerosols, which were included in WRF Chem to represent chemistry in the gas phase, aqueous aerosols, and clouds.

Calculations of OA Viscosity and Particle-Phase Diffusivity. We calculated the viscosity of OA (η_{org}) based on the glass transition temperature of OA ($T_{g,org}$), which is essentially the temperature at which the transition to the amorphous solid phase state occurs.[23] Viscosity was calculated online at each WRF Chem model time step and grid cell as a function of temperature, RH, and OA composition (volatility and O/C ratio), as described in Rasool et al.,[24] and further details of these calculations are provided in the Supporting Information. Calculations of OA viscosity and particle phase diffusivity are performed.

WRF-Chem Model Configuration. Comparing model predictions to measurements of OA is especially challenging over the Amazon rainforest due to uncertainties in the emissions of biogenic volatile organic compounds (VOCs)

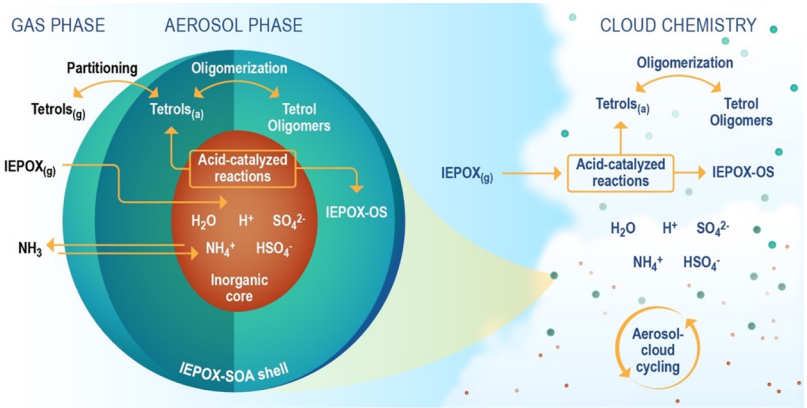

Figure 2. Schematic illustrating the WRF Chem simulated processes governing IEPOX SOA formation due to multiphase chemistry in aqueous aerosol phase (left) and cloud droplets (right). Tetrols and IEPOX OS refer to 2 methyltetrols and organosulfates, which are key components of IEPOX SOA, respectively. IEPOX SOA formed by cloud chemistry becomes part of aerosols after cloud droplets evaporate and could recycle back to clouds.

and a complex wet scavenging environment.[25] We used the regional weather research and forecasting model coupled to the chemistry (WRF Chem 4.2) model[26,27] at high resolution, that is, at 10 km grid spacing, covering 1500 × 1000 km around the Manaus urban area in the Amazon (Supporting Information, WRF Chem setup and Table S3). Inorganic aerosol chemistry in WRF Chem is represented by the Model for Simulating Aerosol Interactions and Chemistry (MOSAIC).[28] SOA formed due to the oxidation of biogenic substances (isoprene and terpenes), biomass burning, and anthropogenic organic gases is represented using our previously documented volatility basis set (VBS) approaches,[18,29,30] which agreed with field measurements over the Amazon.[18,29,30] SOA formation due to the oxidation of VOCs such as isoprene and terpene, which are emitted from both biogenic and biomass burning sources, is implicitly included. Each particle phase chemical constituent is represented by 20 size sections as both interstitial and cloud borne aerosols. We simulate all components of OA (Supporting Information, *Updates to SOA model formulations*). Key developments to the WRF Chem modules used in this study include integrating our recent SOA modules[29] with a radical two dimensional volatility basis set (2D VBS) for monoterpene SOA[18,30] and isoprene SOA from both pure gas phase chemistry (represented by VBS) and multiphase chemistry (IEPOX SOA) pathways.[31] Mechanistic IEPOX SOA formation pathways were developed and included in WRF Chem (Supporting Information, *IEPOX SOA formation*). Total simulated OA includes directly emitted primary anthropogenic and biomass burning OA (POA) and SOA formed due to the atmospheric oxidation of isoprene, monoterpenes, anthropogenic, and biomass burning precursors (represented by VBS approaches). The total OA from all sources is assumed to form an organic shell around the inorganic core, which limits IEPOX SOA formation as a function of the phase state of the OA shell and its viscosity. The variations in viscosity and diffusivity of OA with temperature, RH, volatility, and O/C ratio are also explicitly calculated at each grid cell and time step in WRF Chem (Supporting Information, *Calculations of OA viscosity and particle phase diffusivity*).

Simulated IEPOX-SOA Formation. In this work, we incorporated IEPOX SOA formation into the model by simulating the heterogeneous reactive uptake of gas phase IEPOX on aqueous inorganic seed particles following a resistor model described in Anttila et al.[32] This model accounts for gas phase diffusion, accommodation at the particle surface, diffusion limitations in the organic shell surrounding an aqueous inorganic core, and particle phase chemical reactions (Figure 2), resulting in the formation of methyltetrols and organosulfates as key IEPOX SOA components. Since methyltetrols are semivolatile,[33] we included their measure ment based reversible partitioning between gas and particle phases and their oligomerization to form nonvolatile products.[33] Additionally, we included in cloud IEPOX SOA formation due to the uptake of soluble gases (IEPOX and methyltetrols) in droplets and their washout and removal by precipitation.

Simulated IEPOX SOA (from both in plant and atmos pheric pathways) contributes ∼20% to total OA near the surface and ∼10% in the upper troposphere.

RESULTS AND DISCUSSION

Isoprene Gas and Its Oxidation Products. To under stand IEPOX SOA formation, it is important to evaluate isoprene concentrations simulated with WRF Chem, since models that overestimate isoprene emissions also overpredict IEPOX SOA substantially, for example, as shown in Jo et al.[14] Most measurements used in this study for model evaluation are from the German high altitude and long range research aircraft (HALO)[17] conducted during the ACRIDICON CHUVA measurement campaign.[34] However, HALO did not carry instrumentation to measure isoprene. Therefore, to evaluate isoprene measurements, we used G 159 Gulfstream I (G 1) aircraft[35,36] data. We compared the WRF Chem simulated sum of isoprene and its oxidation products (isoprene hydroxyl hydroperoxide (ISOPOOH) + methyl vinyl ketone + methacrolein) with G 1 aircraft observations using a proton transfer reaction mass spectrometer at 0−2 km altitude near the surface on several days. The Default MEGAN CLM model, used for predicting biogenic emissions in WRF Chem, overestimated the sum of isoprene and its oxidation products by a factor of 3 on average. Therefore, we reduced isoprene emissions by the same factor. After this change, the model agreed with the observed sum of isoprene and its oxidation products near the surface with significantly reduced model measurement biases of 23−35% in their spatially averaged

Table 1. Description of IEPOX SOA Sensitivity Simulations

model ID	description	wet removal	tetrol emission	convective transport	reactive uptake	phase/viscosity of OA
Default	IEPOX-SOA is formed by multiphase atmospheric chemistry	yes	no	yes	yes	varying with T, RH, and OA composition
LiqDorg	same as Default but assuming OA is liquid throughout the atmosphere	yes	no	yes	yes	liquid with a constant particle-phase diffusivity D_{org} 1×10^{-5} cm^2 s^{-1}
nowetremoval	same as Default but with wet removal of aerosols and trace gases turned off	no	no	yes	yes	same as Default
TetrolEmit	Default + the plant emissions source of 2-methyltetrol gases	yes	yes	yes	yes	same as Default
TetrolEmitNoConvTrans	same as TetrolEmit but with cloud convective transport turned off	yes	yes	no	yes	same as Default
highreactiveuptake	same as Default but with 10 times higher IEPOX reactive uptake on aqueous aerosols near the surface	yes	no	yes	yes (but 10 times higher)	same as Default

concentrations (Table S4). Figure S3 shows the simulated daytime spatial variations in isoprene emission fluxes over the Amazon.

Viscosity and Composition of OA. Temperature, RH, and composition govern the spatial variations in the phase state and viscosity of OA (Methods). WRF Chem simulated ambient temperature and RH agree well with measurements onboard HALO, both near the surface (0−2 km) and in the upper troposphere (12−14 km altitude), as shown in Figure 1a,b.

Figure 1c shows the simulated ratio of glass transition temperature (calculations described in the Methods) of OA to the ambient temperature, that is, $T_{g,mix}/T$ ratio. A ratio greater than 1.0 implies an amorphous solid OA, while a ratio less than 0.8 indicates liquid like OA.[37,38] Figure 1c shows that the simulated $T_{g,mix}/T$ ratio at 0−2 km altitude is ∼0.7, suggesting that liquid like OA persists near the surface, mainly due to high RH (∼70%) and warm temperatures (∼300 K) (Figure 1b). In sharp contrast, the simulated $T_{g,mix}/T$ ratio in the upper troposphere is ∼1.1 due to lower RH (∼40%), cold temperatures (∼225 K, Figure 1a), and a dominant contribution of monoterpene SOA to OA (Figure 1d), resulting in a predicted OA viscosity exceeding the 1×10^{12} Pa typical of solids. Several experimental studies have shown that monoterpene SOA exists in a highly viscous or amorphous solid state,[39−41] especially in the cirrus regions of the free troposphere.[42] In addition, IEPOX SOA components including 2 methyltetrols and organosulfates have been found to be highly viscous.[43] Our prediction of solid OA (dominated by monoterpene SOA) in the upper troposphere is consistent with these experimental studies. In addition to the solid OA shell, the inorganic aerosol core was also predicted to be mostly solid in the upper troposphere due to a low prevailing RH (Figure 1b) of ∼40% (below the deliquescence RH of inorganic salt mixtures of ∼80%) at temperatures below 240 K.[44] The solid inorganic core is devoid of particle water and precludes any aqueous phase chemistry. The contrast in the phase state of SOA coating the inorganic shell (liquid near the surface and solid in the upper troposphere) is critical for understanding IEPOX SOA processes as discussed below.

Aircraft Measurements of IEPOX-SOA and Model Predictions. We focus on comparisons between 0−2 km (near the surface) and 10−14 km (upper troposphere) for the following reasons:

(1) Since OA is liquid near the surface and solid in the upper troposphere (Figure 1c), comparing the surface to the upper troposphere provides the clearest contrast in how the OA phase and diffusion limitations affects IEPOX SOA formation.

(2) Mass concentrations observed using HALO for all species decrease rapidly in the middle troposphere (5−8 km altitude);[17] therefore, the signal to noise ratio of the measurements is weakest for this altitude range.

(3) Strong convective updrafts, which transport aerosols and trace gases from the surface to the upper troposphere, are common over the Amazon during the dry season. The convective parameterization used in this study predicts a mixture of cloud tops at low levels (1.5−2.0 km) and deep convection that extends to the upper troposphere (>12 km) during the period of interest, with lesser amounts of clouds at intervening levels (Figure S4). Detrainment primarily occurs near the cloud top for deep convection when mass fluxes increase with height to the near troposphere.[45]

Aircraft measurements showed considerable differences between lower and upper troposphere aerosol mass and number concentrations.[17] Consistent with these measurements, our WRF Chem simulations described below suggest that most of the upper tropospheric IEPOX SOA requires an in situ source.

We compare results from different IEPOX SOA model sensitivity simulations as described in Table 1 with HALO measured average IEPOX SOA[17] for September 21, 2014 (Figure 3). The Default model simulation (blue, Figure 3) representing the current state of knowledge of IEPOX SOA moderately underpredicts the observed IEPOX SOA of ∼0.6 $\mu g\ m^{-3}$ (gray) near the surface (0−2 km altitude) by a factor of 3. However, it greatly underpredicts IEPOX SOA in the upper troposphere by over an order of magnitude (factor of ∼12−22), that is, the measured IEPOX SOA is 0.2−0.4 $\mu g\ m^{-3}$, while the Default simulated value is negligible, ∼0.01−0.03 $\mu g\ m^{-3}$.

In the Default model formulation, IEPOX reactive uptake is negligible at upper troposphere altitudes (10−14 km) since viscosity calculations as a function of temperature, RH, and OA composition predict a solid OA shell due to the cold and moderately dry conditions. The solid OA shell shuts off the reactive uptake of IEPOX. In addition, aqueous and cloud chemistry processes do not occur in the upper troposphere due to low RH (20−40%) and cold temperatures (∼225 K) (Figure 1a,b), which leads to the absence of particle and cloud liquid water needed for aqueous chemistry of IEPOX SOA. In

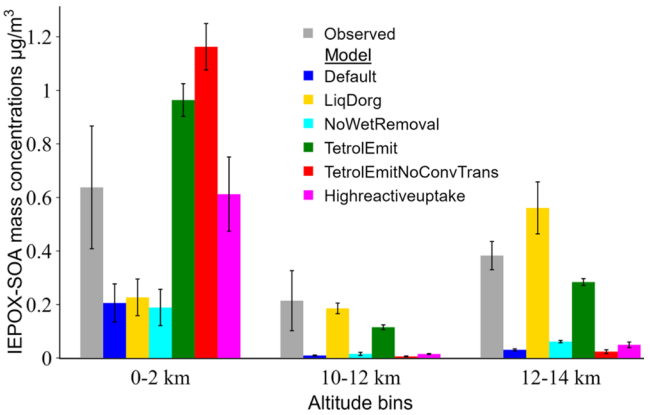

Figure 3. HALO aircraft measured (gray) and WRF Chem simulated (colored) IEPOX SOA mass concentrations (μg m^{-3}, at standard temperature and pressure: 300 K and 995 hPa) are averaged across the same latitude−longitude ranges and times at three altitude ranges, the surface (0−2 km), and upper troposphere (10−12 and 12−14 km), on September 21, 2014. The bars represent averages of IEPOX SOA at each altitude range, while the whiskers denote standard deviations showing the extent of spatial variations.

contrast, the mostly warm and moist near surface conditions (temperature ∼ 300 K, RH ∼ 75%) result in a liquid like OA shell below 2 km altitudes. The Default simulation represents the current state of knowledge in IEPOX SOA formation and shows a key gap in our understanding of IEPOX SOA formation in the upper troposphere.

To assess the impact of OA viscosity and aerosol water on IEPOX SOA formation, we conducted a sensitivity simulation with the OA shell assumed to be liquid (LiqDorg, Table 1). This simulation did not include any primary emissions of 2 methyltetrol gases like the Default simulation. The LiqDorg model formulation (Figure 3, yellow) increases the predicted IEPOX SOA by over an order of magnitude in the upper troposphere compared to the Default simulation. A liquid OA shell greatly increases the kinetics of the uptake of IEPOX gases in particles due to faster bulk diffusion compared to a highly viscous solid OA shell. LiqDorg can explain the observed IEPOX SOA levels in the upper troposphere without plant methyltetrol emissions (Figure 3), however, for physically inaccurate reasons. Previous model formulations that do not account for the role of viscous OA coatings may also predict significant IEPOX SOA formation at high altitudes,[13,15,16] like our LiqDorg formulation. LiqDorg predicts similar IEPOX SOA at near surface altitudes as the Default formulation (within 10%), since high near surface RH causes OA to be liquid like in all model formulations.

Role of Wet Removal of IEPOX-SOA. WRF Chem includes the wet removal of trace gases and aerosols both by grid resolved and parameterized convection. Wet removal decreases IEPOX SOA during their convective transport, since particles can get activated and washed out (removed) by rain. To assess the effects of wet removal of IEPOX SOA during convective transport, we perform a sensitivity simulation with both grid resolved and parameterized convective wet removal processes turned off (Figure 3, NoWetRemoval, cyan). The NoWetRemoval formulation increases IEPOX SOA in the upper troposphere by a factor of ∼2 compared to the Default simulation (Figure 3) but still underpredicts observed IEPOX SOA by an order of magnitude. Therefore, uncertainties in wet removal cannot explain the large underprediction of IEPOX SOA in the upper troposphere.

Increased Reactive Uptake of IEPOX. To assess the effects of uncertainties in reactive uptake kinetics of IEPOX within aqueous phase aerosols, we increased the heterogeneous reactive uptake of IEPOX (Highreactiveuptake, magenta) by an order of magnitude in the Default simulation. Highreactiveuptake increases the simulated IEPOX SOA by a factor of 3 near the surface (0−2 km altitude) and increases upper tropospheric IEPOX SOA by a factor of 1.7 compared to Default (Figure 3). The increase in the upper tropospheric IEPOX SOA is mainly due to the increase in near surface IEPOX SOA and its subsequent transport to the upper troposphere. However, highreactiveuptake still underpredicts upper tropospheric IEPOX SOA by an order of magnitude compared to observations. Therefore, uncertainties in reactive uptake parameterizations of IEPOX SOA cannot account for large model measurement differences in IEPOX SOA in the upper troposphere. Evaluating the model in the upper troposphere provides critical insights into gaps in the traditional understanding of IEPOX SOA processes.

Role of Methyltetrol Emissions from Plants and Their Convective Transport. Direct emissions of gas phase methyltetrols by in plant chemistry and their vertical convective transport represent a previously unconsidered pathway of IEPOX SOA formation. More than 99% of these gases partition to the particle phase OA in the upper troposphere due to extremely cold temperatures (Figure S5b), while at warmer temperatures near the surface, a smaller fraction (50−70%) of these gases exist in the particle phase (Supporting Information, Figure S5a). Consistent with our modeling results, measurements over the Amazon at a surface site reported particle fractions of 2 methyltetrols to be in the range of 40−70%.[46] To assess the role of methyltetrol emissions formed by in plant biochemistry in IEPOX SOA formation, we included primary emissions of methyltetrol gases (TetrolEmit, green) within WRF Chem. We chose the molar emission ratio of 2 methyltetrols to isoprene as 0.5% approaching the lower bound of the reported range of the estimated range of 0.2−3% over the rainforest.[10] The plant biochemical source of 2 methyltetrols is expected to be spatially heterogeneous and vary with plant species and environmental stressors,[10] but additional measurements are needed to quantify this heterogeneity. Here, we assumed methyltetrols to have the same spatial heterogeneity as isoprene emissions (Supporting Information, Figure S3).

Figure 3 shows that the TetrolEmit formulation (green) increases near surface simulated IEPOX SOA by a factor of ∼5 compared to the Default simulation and significantly improves model agreement with aircraft observations. However, the most striking impact of TetrolEmit appears in the upper troposphere, where predicted IEPOX SOA increases by a factor of ∼9−12 compared to the Default formulation and approaches the aircraft observations of ∼0.3 μg m^{-3}. The TetrolEmit formulation moderately overestimates average near surface (0−2 km) IEPOX SOA concentrations by ∼50% relative to HALO and underestimates upper tropospheric IEPOX SOA by 47 and 26% at 10−12 km and 12−14 km altitudes, respectively (Figure 3). The TetrolEmit formulation thus closes the order of magnitude gap between Default model predictions and observations (within a factor of 2). The moderate model measurement biases in the TetrolEmit formulation on different days are likely related to

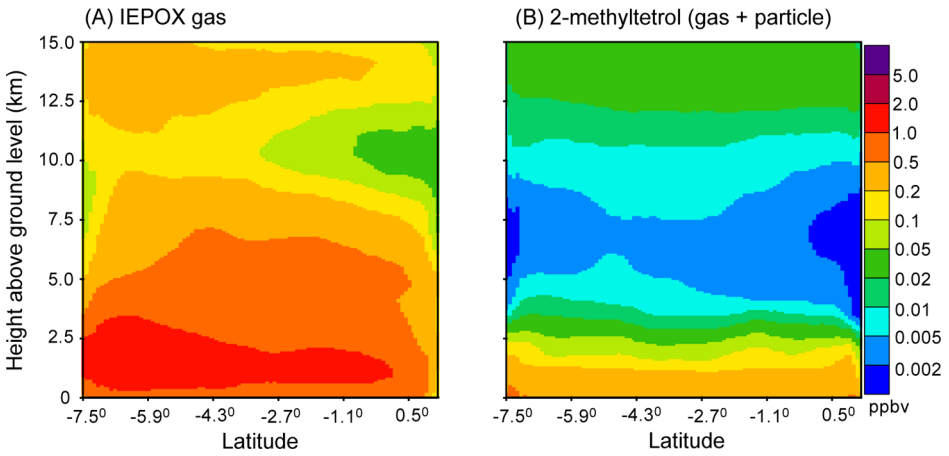

Figure 4. WRF Chem simulated zonal mean vertical distributions during 14−22 UTC on Sep 21−28 over the simulated domain using the TetrolEmit model formulation: (a) IEPOX gas (ppbv) and (b) 2 mehtyltetrol (gas + particle, ppbv). Almost all semivolatile 2 methyltetrol gases condense to particles in the upper troposphere, and the sum of methyltetrols in gas and particle phases represents their total source (from plants and that produced by IEPOX reactive uptake). In the upper troposphere, the plant source constitutes >90% of simulated 2 methyltetrols and IEPOX SOA.

spatial and temporal variations in emissions, convection, and chemistry, which are difficult to represent accurately within the model.

In addition to the upper troposphere, the TetrolEmit formulation suggests that the direct emission source of 2 methyltetrols is likely more important than the traditional multiphase chemistry source near the surface but is not considered in current modeling paradigms. In addition to direct oxidation within leaves due to plant biochemistry, another potential source of 2 methyltetrols is the oxidation of deposited IEPOX gases on the surface of leaves and soils that have water, inorganics, and acidity since IEPOX gas was demonstrated to have rapid dry deposition fluxes.[47]

Note that IEPOX gas concentrations near the surface (produced by atmospheric oxidation of isoprene) are an order of magnitude greater than the concentrations of methyltetrol gases emitted from plants in our simulations (Figure 4). Even in the upper troposphere, the available IEPOX gas concentrations are ∼a factor of 4 higher than methyltetrols since all trace gases and aerosols are transported by deep convection to the upper troposphere. Since IEPOX gas (C^* of 1.7×10^4 μg m^{-3})[33] has ∼3 orders of magnitude higher volatility than 2 methyltetrols ($C^* \sim 10$ μg m^{-3}),[33] IEPOX does not directly partition to aerosols in contrast with 2 methyltetrol gases that undergo gas−particle partitioning. In addition, while IEPOX gas cannot be reactively taken up by particles in the upper troposphere, as explained above, all methyltetrol gases partition to particles due to their semi volatile nature and cold temperatures. Therefore, despite their smaller concentrations compared to IEPOX, methyltetrols are key sources of IEPOX SOA in the upper troposphere due to their semivolatile nature.

Ubiquitous Sources of IEPOX-SOA. On several days (e.g., Sep 21, 23, and 28), the aircraft sampled different locations over the Amazon rainforest and measured significant IEPOX SOA (∼0.2−0.5 μg m^{-3}) in the upper troposphere with higher concentrations near the surface (Figures 3 and S2 and Table S5). Measurements show a ubiquitous source of IEPOX SOA near the surface and upper troposphere. Without the emissions of methyltetrols from leaves/soils and their gas−particle partitioning, it is difficult to explain the ubiquitous upper tropospheric source of IEPOX SOA, as described above.

We note that some of the condensed particle phase methyltetrols may evaporate as they pass through the aircraft particle inlet and AMS (mounted within the aircraft, behind a particle inlet) at high altitudes; thus, their upper tropospheric concentrations are likely higher than measurements. Account ing for this measurement bias would likely require higher methyltetrol emissions, while this study used a lower bound estimate (Figure 3).

Convective Transport of Methyltetrols to the upper Troposphere. To determine if the vertical convective transport of methyltetrol gases to the upper troposphere is critical for model measurement agreement in IEPOX SOA, we conducted another sensitivity simulation where methyltetrol gases were emitted by plants but the subgrid scale convective transport of aerosols and trace gases was turned off (TetrolEmitNoConvTrans). This formulation decreases simu lated IEPOX SOA in the upper troposphere by a factor of ∼10−20 compared to the TetrolEmit formulation (Figure 3, red). Therefore, without the vertical convective transport, direct plant emissions of methyltetrols do not contribute to upper tropospheric IEPOX SOA. Our results showing the role of cloud updrafts in transporting SOA precursors from the surface to the upper troposphere are consistent with aircraft measurements in the Amazon.[17−19]

Transport of Other SOA Precursors to the upper Troposphere. Similar to IEPOX SOA, we found that other SOA components (including monoterpene SOA) decrease substantially in the upper troposphere when convective transport is turned off. Figure S6 compares total simulated OA (POA + SOA) from TetrolEmit and TetrolEmitNoConv Trans simulations with HALO AMS observations. While the TetrolEmit formulation (green) agrees well with observations at all altitudes, turning off the convective transport causes the model to greatly underestimate total OA in the upper troposphere (red). Thus, deep convective transport plays a key role in coupling SOA precursors emitted near the surface to their formation in the upper troposphere.

Ratio of IEPOX-SOA to Total OA. It is also instructive to evaluate the simulated ratios of IEPOX SOA to total OA from

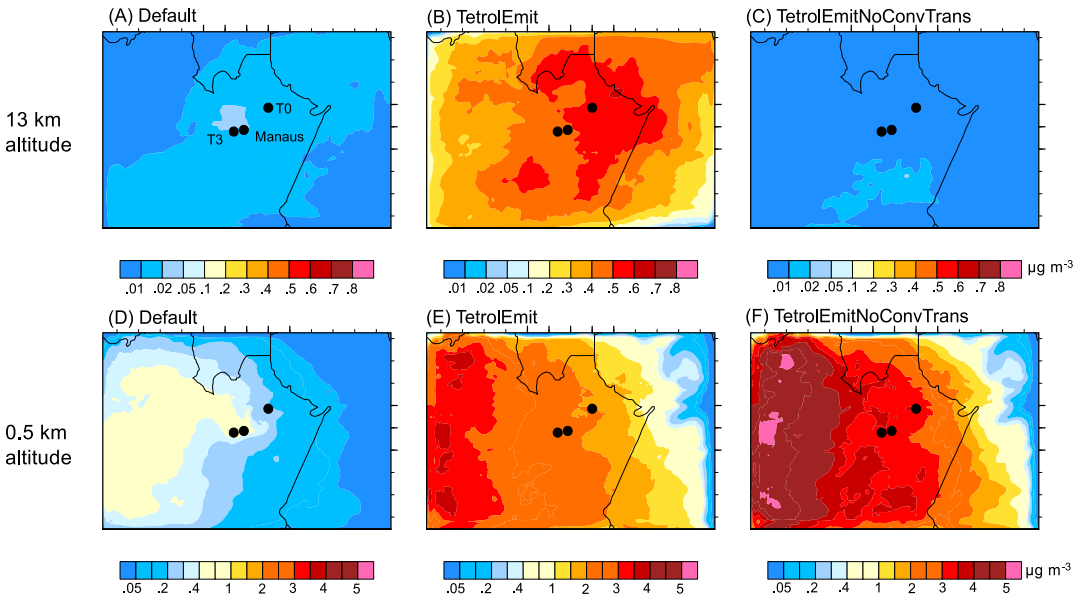

Figure 5. WRF Chem simulated IEPOX SOA spatial distributions. IEPOX SOA concentrations (μg m^{-3} under standard conditions: 300 K and 995 hPa) near the surface (~0.5 km altitude, bottom panels) and upper troposphere (~13 km altitude, top panels) during the daytime 14–22 UTC during September 21–28, 2014. The locations of the background T0 and urban influenced Manaus and T3 sites are shown as black dots. Color scales on top and bottom panels are different to show the spatial variations.

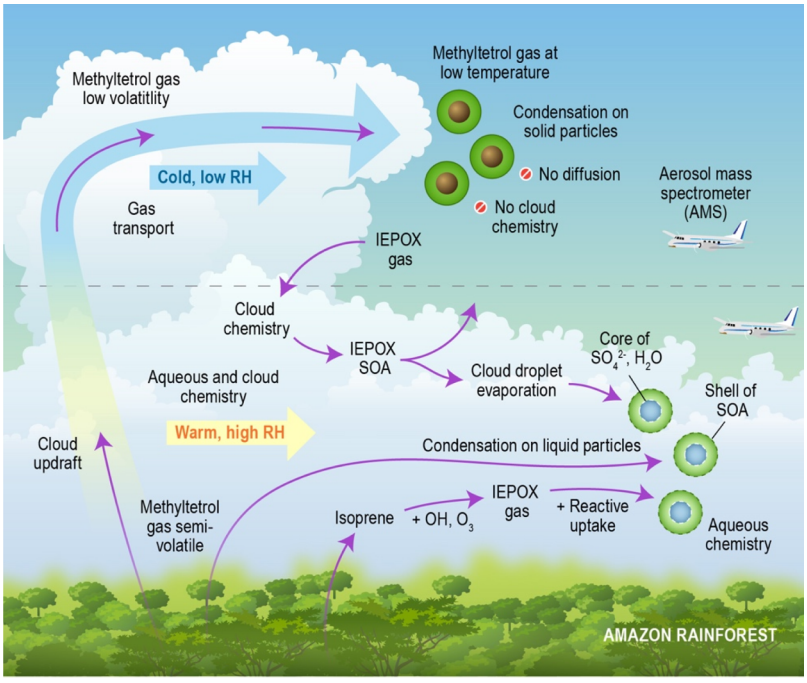

Figure 6. Illustration of the effect of in plant oxidation of isoprene on IEPOX SOA formation. Near the surface, the reactive uptake of IEPOX on liquid aerosols contributes to IEPOX SOA formation in addition to direct emissions of methyltetrols, but at high altitudes in the upper troposphere, IEPOX SOA does not form by this multiphase reactive uptake since particles are solid, imposing strong diffusion limitations, and liquid water needed for aqueous chemistry is absent at low RH in the upper troposphere. Release of methyltetrols through in plant oxidation of isoprene and/or oxidation of deposited IEPOX on leaves/soils can directly emit semivolatile methyltetrol gases, which are transported by deep convective updrafts to the upper troposphere. Due to cold temperatures in the upper troposphere, all the semivolatile methyltetrol gases condense to aerosols and explain the measurements conducted by the HALO aircraft.

HALO AMS measurements. These observations suggest that IEPOX SOA constitutes 23% of total OA (measured by AMS) at 0–2 km altitudes and 12–15% of OA at 10–14 km on September 21, 2014 (Figures 1d and S2). The Default formulation severely underpredicts this ratio by factors of 12–14 between 10 and 14 km and underpredicts it by a factor of ~4 near the surface (Supporting Information, Table S5). The TetrolEmit model formulation shows excellent agreement with the observed IEPOX SOA to OA ratio (simulated and predicted values of 0.23) near the surface and moderately underpredicts it by a factor of ~1.5 at 10–14 km altitudes (Figures 1d and S2 and Table S5).

Spatial Distribution of Simulated IEPOX-SOA. Figure 5 shows the spatial distribution of simulated IEPOX SOA for the Default, TetrolEmit, and TetrolEmitNoConvTrans model formulations near the surface (bottom panels) and in the upper troposphere (top panels) averaged during the daytime (14−22 UTC) on September 21−28, 2014. Domain wide, the Default formulation predicts IEPOX SOA concentrations are at least an order of magnitude lower in the upper troposphere (Figure 5a) than the surface (Figure 5d). Near the surface, IEPOX SOA is higher over and downwind the Manaus regions, where higher aerosol concentrations favor the IEPOX uptake. The TetrolEmit model formulation predicts an order of magnitude higher IEPOX SOA compared to Default (Figure 5b) in the upper troposphere. Near the surface, methyltetrol emissions from plants constitute a background source over a wider spatial extent compared to the Default formulation, consistent with aircraft measurements (Figure 5e). The TetrolEmitNoConvTrans predicts much lower IEPOX SOA in the upper troposphere (Figure 5c) due to the absence of convective transport of methyltetrol gases but predicts higher IEPOX SOA concentrations near the surface (Figure 5f) due to accumulation of SOA precursors that are not transported to the upper troposphere. Figure S7 shows the zonal mean vertical distributions of IEPOX SOA simulated by the Default, TetrolEmit, and TetrolEmitNoConvTrans and NoWetRemoval formulations. Consistent with the spatial plots in Figure 5, the TetrolEmit model formulation produces much higher IEPOX SOA both near the surface and the upper troposphere compared to the Default formulation.

CONCLUSIONS

The vast tropical rainforest of the Amazon undergoes many coupled processes encompassing interactions between the biosphere, atmospheric chemistry, aerosols, clouds, and convective transport. In plant biochemical oxidation of VOCs like isoprene represents a key pathway that could greatly impact aerosol−cloud interactions but is poorly understood. While previous studies have overpredicted IEPOX SOA formation despite their exclusion of direct emissions of methyltetrols, we find that the exclusion of diffusion limitations within organic coatings and/or too high isoprene emissions resulted in significant model biases in previous studies.[13,15,16] We show that in the upper troposphere, the absence of aerosol and cloud liquid water and the prevailing solid phase of aerosols under relatively cold and dry conditions inhibit the reactive uptake of IEPOX by inorganic aerosols. Thus, the Default model simulation predicts an order of magnitude lower IEPOX SOA than observed, revealing a large gap in the traditional understanding of its formation. We resolve this discrepancy by introducing direct emissions of 2 methyltetrol gases likely formed due to in plant biochemistry and/or through the oxidation of IEPOX deposited on leaves/soils, followed by their convective transport and subsequent condensation in the upper troposphere.

Figure 6 schematically illustrates our results, which imply that in plant biochemistry and/or oxidation of IEPOX on the surface of acidic media such as leaves/soils represents a key unaccounted source of semivolatile gases that interact with atmospheric aerosols and clouds. While our current study focuses on IEPOX SOA, there is clear evidence that inplant biochemistry causes emissions of other compounds as well (e.g., methyl vinylketone and methacrolein), which were assumed to be produced only by oxidation of isoprene in the atmosphere.[4] Combining aircraft measurements and detailed modeling, we showed that clouds and convective transport couple the surface level biosphere to the upper troposphere and that the upper tropospheric SOA formation provides critical clues for key biosphere processes, which have not been considered previously.

ASSOCIATED CONTENT

Supporting Information

The Supporting Information is available free of charge at https://pubs.acs.org/doi/10.1021/acsearthspacechem.1c00356.

Detailed sections on the WRF Chem model setup, WRF Chem inputs including emissions of trace gases and particles, biogenic and biomass burning emissions, model treatments of gas phase chemistry, aerosol particle treatments, model formulations of SOA processes including IEPOX SOA formation within aerosol particles and clouds, calculations of OA viscosity and particle phase bulk diffusivity, details of HALO aircraft based observational estimates of IEPOX SOA, WRF Chem domain, observed and modeled domain averaged OA components, daytime isoprene emission fluxes, WRF Chem simulated cloud top heights, WRF Chem simulated particle fraction of 2 methyltetrols, HALO observed and WRF Chem simulated total OA at three altitude ranges, WRF Chem simulated zonal average concentrations of IEPOX SOA, gas phase IEPOX SOA reactions, rate constants for aqueous IEPOX SOA, WRF Chem configuration, observed and simulated isoprene concentrations, observed and simulated IEPOX SOA concentrations, and VBS parameters representing biomass burning SOA formation (PDF)

AUTHOR INFORMATION

Corresponding Author

Manish Shrivastava − *Pacific Northwest National Laboratory, Richland, Washington 993522, United States;* orcid.org/0000 0002 9053 2400;
Email: ManishKumar.Shrivastava@pnnl.gov

Authors

Quazi Z. Rasool − *Pacific Northwest National Laboratory, Richland, Washington 993522, United States;* orcid.org/0000 0001 6274 6236

Bin Zhao − *Pacific Northwest National Laboratory, Richland, Washington 993522, United States;* Present Address: State Key Joint Laboratory of Environmental Simulation and Pollution Control, School of Environment, Tsinghua University, Beijing 100084, China; orcid.org/0000 0001 8438 9188

Mega Octaviani − *Pacific Northwest National Laboratory, Richland, Washington 993522, United States;* Present Address: Institute of Meteorology and Climate Research, Department of Troposphere Research, Karlsruhe Institute of Technology, Eggenstein Leopoldshafen 76344, Germany.

Rahul A. Zaveri − *Pacific Northwest National Laboratory, Richland, Washington 993522, United States;* orcid.org/0000 0001 9874 8807

Alla Zelenyuk − *Pacific Northwest National Laboratory, Richland, Washington 993522, United States*

Brian Gaudet − *Pacific Northwest National Laboratory, Richland, Washington 993522, United States*
Ying Liu − *Pacific Northwest National Laboratory, Richland, Washington 993522, United States*
John E. Shilling − *Pacific Northwest National Laboratory, Richland, Washington 993522, United States;* orcid.org/0000 0002 3728 0195
Johannes Schneider − *Particle Chemistry Department, Max Planck Institute for Chemistry, Mainz 55128, Germany*
Christiane Schulz − *Experimental Aerosol and Cloud Microphysics Department, Leibniz Institute for Tropospheric Research, Leipzig 04318, Germany; Particle Chemistry Department, Max Planck Institute for Chemistry, Mainz 55128, Germany;* Present Address: Leibniz Centre for Agricultural Landscape Research; Müncheberg 15374, Germany.
Martin Zöger − *Flight Experiments, German Aerospace Center (DLR), Oberpfaffenhofen 82234, Germany*
Scot T. Martin − *School of Engineering and Applied Sciences and Department of Earth and Planetary Sciences, Harvard University, Cambridge, Massachusetts 02138, United Staes;* orcid.org/0000 0002 8996 7554
Jianhuai Ye − *School of Engineering and Applied Sciences and Department of Earth and Planetary Sciences, Harvard University, Cambridge, Massachusetts 02138, United Staes;* Present Address: School of Environmental Science and Engineering, Southern University of Science and Technology; Shenzhen, Guangdong, 518055, China.; orcid.org/0000 0002 9063 3260
Alex Guenther − *Department of Earth System Science, University of California Irvine, Irvine, California 92697, United States*
Rodrigo F. Souza − *Superior School of Technology, Amazonas State University, Manaus, Amazonas 69050020, Brazil*
Manfred Wendisch − *Leipzig Institute for Meteorology, University of Leipzig, Leipzig 04103, Germany*
Ulrich Pöschl − *Multiphase Chemistry Department, Max Planck Institute for Chemistry, Mainz 55128, Germany;* orcid.org/0000 0003 1412 3557

Complete contact information is available at: https://pubs.acs.org/10.1021/acsearthspacechem.1c00356

Author Contributions

Design, conceptualization, and model simulations: M.S. Data analyses: M.S., Q.Z.R., B.Z., B.G., J.E.S, R.A.Z, A.Z., C.S., and J.S. Visualizations: M.S. and Q.Z.R. Processing of emissions: Y.L. Project administration and supervision: M.S. Writing: all co authors.

Notes

The authors declare no competing financial interest.
All data analyzed during the current study are included in this published article and its Supporting Information Measured data during the GoAmazon2014/5 field campaign are publicly available on the Atmospheric Radiation Measurement (ARM) website: https://www.arm.gov/research/campaigns/amf2014goamazon. The ACRIDICN CHUVA data of HALO can be obtained from the HALO database https://halo db.pa.op.dlr.de/. Raw model simulations from WRF Chem are available from the corresponding author on reasonable request.

■ ACKNOWLEDGMENTS

This research was supported by the U.S. Department of Energy (DOE) Office of Science, Office of Biological and Environ mental Research (BER) through the Early Career Research Program and DOE BER's Atmospheric System Research (ASR) program. Funding for data collection onboard the G 1 aircraft and at the ground sites was provided by the Atmospheric Radiation Measurement (ARM) Climate Re search Facility, a DOE user facility sponsored by BER. HALO related work was supported by the Max Planck Society, the DFG (Deutsche Forschungsgemeinschaft, German Research Foundation) Priority Program SPP 1294, the German Aerospace Center (DLR), the BMBF program ROMIC (01LG1205E), the Max Planck Society, the Brazilian foundations FAPESP (São Paulo Research Foundation) Grants 2009/15235 8 and 2013/05014 0 and FAPEAM, and a wide range of other institutional partners. The Pacific Northwest National Laboratory (PNNL) is operated for the DOE by Battelle Memorial Institute under contract DE AC06 76RL01830. Computational resources for the simulations were provided by EMSL (a DOE Office of Science User Facility sponsored by the Office of Biological and Environ mental Research located at PNNL).

■ REFERENCES

(1) Guenther, A. B.; Jiang, X.; Heald, C. L.; Sakulyanontvittaya, T.; Duhl, T.; Emmons, L. K.; Wang, X. The Model of Emissions of Gases and Aerosols from Nature version 2.1 (MEGAN2.1): an extended and updated framework for modeling biogenic emissions. *Geosci. Model Dev.* **2012**, *5*, 1471−1492.
(2) Carlton, A. G.; Wiedinmyer, C.; Kroll, J. H. A review of Secondary Organic Aerosol (SOA) formation from isoprene. *Atmos. Chem. Phys.* **2009**, *9*, 4987−5005.
(3) Shrivastava, M.; Cappa, C. D.; Fan, J.; Goldstein, A. H.; Guenther, A. B.; Jimenez, J. L.; Kuang, C.; Laskin, A.; Martin, S. T.; Ng, N. L.; Petaja, T.; Pierce, J. R.; Rasch, P. J.; Roldin, P.; Seinfeld, J. H.; Shilling, J.; Smith, J. N.; Thornton, J. A.; Volkamer, R.; Wang, J.; Worsnop, D. R.; Zaveri, R. A.; Zelenyuk, A.; Zhang, Q. Recent advances in understanding secondary organic aerosol: Implications for global climate forcing. *Rev. Geophys.* **2017**, *55*, 509−559.
(4) Jardine, K. J.; Monson, R. K.; Abrell, L.; Saleska, S. R.; Arneth, A.; Jardine, A.; Ishida, F. Y.; Serrano, A. M. Y.; Artaxo, P.; Karl, T.; Fares, S.; Goldstein, A.; Loreto, F.; Huxman, T. Within plant isoprene oxidation confirmed by direct emissions of oxidation products methyl vinyl ketone and methacrolein. *Global Change Biol.* **2012**, *18*, 973−984.
(5) Surratt, J. D.; Chan, A. W. H.; Eddingsaas, N. C.; Chan, M.; Loza, C. L.; Kwan, A. J.; Hersey, S. P.; Flagan, R. C.; Wennberg, P. O.; Seinfeld, J. H. Reactive intermediates revealed in secondary organic aerosol formation from isoprene. *Proc. Natl. Acad. Sci. U.S.A.* **2010**, *107*, 6640−6645.
(6) Ervens, B.; Turpin, B. J.; Weber, R. J. Secondary organic aerosol formation in cloud droplets and aqueous particles (aqSOA): a review of laboratory, field and model studies. *Atmos. Chem. Phys.* **2011**, *11*, 11069−11102.
(7) Claeys, M.; Graham, B.; Vas, G.; Wang, W.; Vermeylen, R.; Pashynska, V.; Cafmeyer, J.; Guyon, P.; Andreae, M. O.; Artaxo, P.; Maenhaut, W. Formation of secondary organic aerosols through photooxidation of isoprene. *Science* **2004**, *303*, 1173−1176.
(8) Hu, W. W.; Campuzano Jost, P.; Palm, B. B.; Day, D. A.; Ortega, A. M.; Hayes, P. L.; Krechmer, J. E.; Chen, Q.; Kuwata, M.; Liu, Y. J.; de Sá, S. S.; McKinney, K.; Martin, S. T.; Hu, M.; Budisulistiorini, S. H.; Riva, M.; Surratt, J. D.; St. Clair, J. M.; Isaacman Van Wertz, G.; Yee, L. D.; Goldstein, A. H.; Carbone, S.; Brito, J.; Artaxo, P.; de Gouw, J. A.; Koss, A.; Wisthaler, A.; Mikoviny, T.; Karl, T.; Kaser, L.; Jud, W.; Hansel, A.; Docherty, K. S.; Alexander, M. L.; Robinson, N.

H.; Coe, H.; Allan, J. D.; Canagaratna, M. R.; Paulot, F.; Jimenez, J. L. Characterization of a real time tracer for isoprene epoxydiols derived secondary organic aerosol (IEPOX SOA) from aerosol mass spectrometer measurements. *Atmos. Chem. Phys.* **2015**, *15*, 11807−11833.
(9) Tsui, W. G.; Woo, J. L.; McNeill, V. F. Impact of Aerosol Cloud Cycling on Aqueous Secondary Organic Aerosol Formation. *Atmosphere* **2019**, *10*, 666.
(10) Ye, J.; Batista, C. E.; Guimarães, P. C.; Ribeiro, I. O.; Vidoudez, C.; Barbosa, R. G.; Oliveira, R. L.; Ma, Y.; Jardine, K. J.; Surratt, J. D.; Guenther, A. B.; Souza, R. A. F.; Martin, S. T. Near canopy horizontal concentration heterogeneity of semivolatile oxygenated organic compounds and implications for 2 methyltetrols primary emissions. *Environ. Sci.: Atmos.* **2021**, *1*, 8−20.
(11) Gaston, C. J.; Riedel, T. P.; Zhang, Z.; Gold, A.; Surratt, J. D.; Thornton, J. A. Reactive Uptake of an Isoprene Derived Epoxydiol to Submicron Aerosol Particles. *Environ. Sci. Technol.* **2014**, *48*, 11178−11186.
(12) Zhang, Y.; Chen, Y.; Lei, Z.; Olson, N. E.; Riva, M.; Koss, A. R.; Zhang, Z.; Gold, A.; Jayne, J. T.; Worsnop, D. R.; Onasch, T. B.; Kroll, J. H.; Turpin, B. J.; Ault, A. P.; Surratt, J. D. Joint Impacts of Acidity and Viscosity on the Formation of Secondary Organic Aerosol from Isoprene Epoxydiols (IEPOX) in Phase Separated Particles. *ACS Earth Space Chem.* **2019**, *3*, 2646−2658.
(13) Bates, K. H.; Jacob, D. J. A new model mechanism for atmospheric oxidation of isoprene: global effects on oxidants, nitrogen oxides, organic products, and secondary organic aerosol. *Atmos. Chem. Phys.* **2019**, *19*, 9613−9640.
(14) Jo, D. S.; Hodzic, A.; Emmons, L. K.; Tilmes, S.; Schwantes, R. H.; Mills, M. J.; Campuzano Jost, P.; Hu, W.; Zaveri, R. A.; Easter, R. C.; Singh, B.; Lu, Z.; Schulz, C.; Schneider, J.; Shilling, J. E.; Wisthaler, A.; Jimenez, J. L. Future changes in isoprene epoxydiol derived secondary organic aerosol (IEPOX SOA) under the Shared Socioeconomic Pathways: the importance of physicochemical dependency. *Atmos. Chem. Phys.* **2021**, *21*, 3395−3425.
(15) Pai, S. J.; Heald, C. L.; Pierce, J. R.; Farina, S. C.; Marais, E. A.; Jimenez, J. L.; Campuzano Jost, P.; Nault, B. A.; Middlebrook, A. M.; Coe, H.; Shilling, J. E.; Bahreini, R.; Dingle, J. H.; Vu, K. An evaluation of global organic aerosol schemes using airborne observations. *Atmos. Chem. Phys.* **2020**, *20*, 2637−2665.
(16) Stadtler, S.; Kühn, T.; Schröder, S.; Taraborrelli, D.; Schultz, M. G.; Kokkola, H. Isoprene derived secondary organic aerosol in the global aerosol−chemistry−climate model ECHAM6.3.0−HAM2.3−MOZ1.0. *Geosci. Model Dev.* **2018**, *11*, 3235−3260.
(17) Schulz, C.; Schneider, J.; Amorim Holanda, B.; Appel, O.; Costa, A.; de Sá, S. S.; Fütterer, D.; Jurkat Witschas, T.; Klimach, T.; Knote, C.; Krämer, M.; Martin, S. T.; Mertes, S.; Pöhlker, M. L.; Sauer, D.; Voigt, C.; Walser, A.; Weinzierl, B.; Ziereis, H.; Zöger, M.; Andreae, M. O.; Artaxo, P.; Machado, L. A. T.; Pöschl, U.; Wendisch, M.; Borrmann, S.; Borrmann, S. Aircraft based observations of isoprene epoxydiol derived secondary organic aerosol (IEPOX SOA) in the tropical upper troposphere over the Amazon region. *Atmos. Chem. Phys.* **2018**, *18*, 14979−15001.
(18) Zhao, B.; Shrivastava, M.; Donahue, N. M.; Gordon, H.; Schervish, M.; Shilling, J. E.; Zaveri, R. A.; Wang, J.; Andreae, M. O.; Zhao, C.; Gaudet, B.; Liu, Y.; Fan, J.; Fast, J. D. High concentration of ultrafine particles in the Amazon free troposphere produced by organic new particle formation. *Proc. Natl. Acad. Sci. U.S.A.* **2020**, *117*, 25344−25351.
(19) Andreae, M. O.; Afchine, A.; Albrecht, R.; Holanda, B. A.; Artaxo, P.; Barbosa, H. M. J.; Borrmann, S.; Cecchini, M. A.; Costa, A.; Dollner, M.; Fütterer, D.; Järvinen, E.; Jurkat, T.; Klimach, T.; Konemann, T.; Knote, C.; Krämer, M.; Krisna, T.; Machado, L. A. T.; Mertes, S.; Minikin, A.; Pöhlker, C.; Pöhlker, M. L.; Pöschl, U.; Rosenfeld, D.; Sauer, D.; Schlager, H.; Schnaiter, M.; Schneider, J.; Schulz, C.; Spanu, A.; Sperling, V. B.; Voigt, C.; Walser, A.; Wang, J.; Weinzierl, B.; Wendisch, M.; Ziereis, H. Aerosol characteristics and particle production in the upper troposphere over the Amazon Basin. *Atmos. Chem. Phys.* **2018**, *18*, 921−961.
(20) González, N. J. D.; Borg Karlson, A. K.; Artaxo, P.; Guenther, A.; Krejci, R.; Nozière, B.; Noone, K. Primary and secondary organics in the tropical Amazonian rainforest aerosols: chiral analysis of 2 methyltetraols. *Environ. Sci.: Processes Impacts* **2014**, *16*, 1413−1421.
(21) Mei, F.; Wang, J.; Comstock, J. M.; Weigel, R.; Krämer, M.; Mahnke, C.; Shilling, J. E.; Schneider, J.; Schulz, C.; Long, C. N.; Wendisch, M.; Machado, L. A. T.; Schmid, B.; Krisna, T.; Pekour, M.; Hubbe, J.; Giez, A.; Weinzierl, B.; Zoeger, M.; Pöhlker, M. L.; Schlager, H.; Cecchini, M. A.; Andreae, M. O.; Martin, S. T.; de Sá, S. S.; Tomlinson, J.; Springston, S.; Pöschl, U.; Artaxo, P.; Pöhlker, C.; Klimach, T.; Minikin, A.; Afchine, A.; Borrmann, S.; Borrmann, S. Comparison of aircraft measurements during GoAmazon2014/5 and ACRIDICON CHUVA. *Atmos. Meas. Tech.* **2020**, *13*, 661−684.
(22) Octaviani, M.; Shrivastava, M.; Zaveri, R. A.; Zelenyuk, A.; Zhang, Y.; Rasool, Q. Z.; Bell, D. M.; Riva, M.; Glasius, M.; Surratt, J. D. Modeling the Size Distribution and Chemical Composition of Secondary Organic Aerosols during the Reactive Uptake of Isoprene Derived Epoxydiols under Low Humidity Condition. *ACS Earth Space Chem.* **2021**, *5*, 3247−3257.
(23) Koop, T.; Bookhold, J.; Shiraiwa, M.; Pöschl, U. Glass transition and phase state of organic compounds: dependency on molecular properties and implications for secondary organic aerosols in the atmosphere. *Phys. Chem. Chem. Phys.* **2011**, *13*, 19238−19255.
(24) Rasool, Q. Z.; Shrivastava, M.; Octaviani, M.; Zhao, B.; Gaudet, B.; Liu, Y. Modeling Volatility Based Aerosol Phase State Predictions in the Amazon Rainforest. *ACS Earth Space Chem.* **2021**, *5*, 2910−2924.
(25) Gordon, H.; Sengupta, K.; Rap, A.; Duplissy, J.; Frege, C.; Williamson, C.; Heinritzi, M.; Simon, M.; Yan, C.; Almeida, J.; Tröstl, J.; Nieminen, T.; Ortega, I. K.; Wagner, R.; Dunne, E. M.; Adamov, A.; Amorim, A.; Bernhammer, A. K.; Bianchi, F.; Breitenlechner, M.; Brilke, S.; Chen, X.; Craven, J. S.; Dias, A.; Ehrhart, S.; Fischer, L.; Flagan, R. C.; Franchin, A.; Fuchs, C.; Guida, R.; Hakala, J.; Hoyle, C. R.; Jokinen, T.; Junninen, H.; Kangasluoma, J.; Kim, J.; Kirkby, J.; Krapf, M.; Kürten, A.; Laaksonen, A.; Lehtipalo, K.; Makhmutov, V.; Mathot, S.; Molteni, U.; Monks, S. A.; Onnela, A.; Peräkylä, O.; Piel, F.; Petäjä, T.; Praplan, A. P.; Pringle, K. J.; Richards, N. A. D.; Rissanen, M. P.; Rondo, L.; Sarnela, N.; Schobesberger, S.; Scott, C. E.; Seinfeld, J. H.; Sharma, S.; Sipilä, M.; Steiner, G.; Stozhkov, Y.; Stratmann, F.; Tomé, A.; Virtanen, A.; Vogel, A. L.; Wagner, A. C.; Wagner, P. E.; Weingartner, E.; Wimmer, D.; Winkler, P. M.; Ye, P.; Zhang, X.; Hansel, A.; Dommen, J.; Donahue, N. M.; Worsnop, D. R.; Baltensperger, U.; Kulmala, M.; Curtius, J.; Carslaw, K. S. Reduced anthropogenic aerosol radiative forcing caused by biogenic new particle formation. *Proc. Natl. Acad. Sci. U.S.A.* **2016**, *113*, 12053−12058.
(26) Fast, J. D.; Gustafson, W. I.; Easter, R. C.; Zaveri, R. A.; Barnard, J. C.; Chapman, E. G.; Grell, G. A.; Peckham, S. E. Evolution of ozone, particulates, and aerosol direct radiative forcing in the vicinity of Houston using a fully coupled meteorology chemistry aerosol model. *J. Geophys. Res.: Atmos.* **2006**, *111*, D21305.
(27) Grell, G. A.; Peckham, S. E.; Schmitz, R.; McKeen, S. A.; Frost, G.; Skamarock, W. C.; Eder, B. Fully coupled "online" chemistry within the WRF model. *Atmos. Environ.* **2005**, *39*, 6957−6975.
(28) Zaveri, R. A.; Easter, R. C.; Fast, J. D.; Peters, L. K. Model for Simulating Aerosol Interactions and Chemistry (MOSAIC). *J. Geophys. Res.: Atmos.* **2008**, *113*, D13204.
(29) Shrivastava, M.; Andreae, M. O.; Artaxo, P.; Barbosa, H. M. J.; Berg, L. K.; Brito, J.; Ching, J.; Easter, R. C.; Fan, J.; Fast, J. D.; Feng, Z.; Fuentes, J. D.; Glasius, M.; Goldstein, A. H.; Alves, E. G.; Gomes, H.; Gu, D.; Guenther, A.; Jathar, S. H.; Kim, S.; Liu, Y.; Lou, S.; Martin, S. T.; McNeill, V. F.; Medeiros, A.; de Sá, S. S.; Springston, S. R.; Souza, R. A. F.; Thornton, J. A.; Isaacman VanWertz, G.; Yee, L. D.; Ynoue, R.; Zaveri, R. A.; Zelenyuk, A.; Zhao, C.; Zhao, C. Urban pollution greatly enhances formation of natural aerosols over the Amazon rainforest. *Nat. Commun.* **2019**, *10*, 1046.
(30) Zhao, B.; Fast, J. D.; Donahue, N. M.; Shrivastava, M.; Schervish, M.; Shilling, J. E.; Gordon, H.; Wang, J.; Gao, Y.; Zaveri, R. A.; Liu, Y.; Gaudet, B. Impact of Urban Pollution on Organic

Mediated New Particle Formation and Particle Number Concentration in the Amazon Rainforest. *Environ. Sci. Technol.* **2021**, *55*, 4357.
(31) Thornton, J. A.; Shilling, J. E.; Shrivastava, M.; D'Ambro, E. L.; Zawadowicz, M. A.; Liu, J. A Near Explicit Mechanistic Evaluation of Isoprene Photochemical Secondary Organic Aerosol Formation and Evolution: Simulations of Multiple Chamber Experiments with and without Added NOx. *ACS Earth Space Chem.* **2020**, *4*, 1161−1181.
(32) Anttila, T.; Kiendler Scharr, A.; Tillmann, R.; Mentel, T. F. On the reactive uptake of gaseous compounds by organic coated aqueous aerosols: Theoretical analysis and application to the heterogeneous hydrolysis of N2O5. *J. Phys. Chem. A* **2006**, *110*, 10435−10443.
(33) D'Ambro, E. L.; Schobesberger, S.; Gaston, C. J.; Lopez Hilfiker, F. D.; Lee, B. H.; Liu, J.; Zelenyuk, A.; Bell, D.; Cappa, C. D.; Helgestad, T.; Li, Z.; Guenther, A.; Wang, J.; Wise, M.; Caylor, R.; Surratt, J. D.; Riedel, T.; Hyttinen, N.; Salo, V. T.; Hasan, G.; Kurtén, T.; Shilling, J. E.; Thornton, J. A. Chamber based insights into the factors controlling epoxydiol (IEPOX) secondary organic aerosol (SOA) yield, composition, and volatility. *Atmos. Chem. Phys.* **2019**, *19*, 11253−11265.
(34) Wendisch, M.; Pöschl, U.; Andreae, M. O.; Machado, L. A. T.; Albrecht, R.; Schlager, H.; Rosenfeld, D.; Martin, S. T.; Abdelmonem, A.; Afchine, A.; Araùjo, A. C.; Artaxo, P.; Aufmhoff, H.; Barbosa, H. M. J.; Borrmann, S.; Braga, R.; Buchholz, B.; Cecchini, M. A.; Costa, A.; Curtius, J.; Dollner, M.; Dorf, M.; Dreiling, V.; Ebert, V.; Ehrlich, A.; Ewald, F.; Fisch, G.; Fix, A.; Frank, F.; Fütterer, D.; Heckl, C.; Heidelberg, F.; Hüneke, T.; Jäkel, E.; Järvinen, E.; Jurkat, T.; Kanter, S.; Kästner, U.; Kenntner, M.; Kesselmeier, J.; Klimach, T.; Knecht, M.; Kohl, R.; Kölling, T.; Krämer, M.; Krüger, M.; Krisna, T. C.; Lavric, J. V.; Longo, K.; Mahnke, C.; Manzi, A. O.; Mayer, B.; Mertes, S.; Minikin, A.; Molleker, S.; Münch, S.; Nillius, B.; Pfeilsticker, K.; Pöhlker, C.; Roiger, A.; Rose, D.; Rosenow, D.; Sauer, D.; Schnaiter, M.; Schneider, J.; Schulz, C.; de Souza, R. A. F.; Spanu, A.; Stock, P.; Vila, D.; Voigt, C.; Walser, A.; Walter, D.; Weigel, R.; Weinzierl, B.; Werner, F.; Yamasoe, M. A.; Ziereis, H.; Zinner, T.; Zöger, M. ACRIDICON CHUVA CAMPAIGN Studying Tropical Deep Convective Clouds and Precipitation over Amazonia Using the New German Research Aircraft HALO. *Bull. Am. Meteorol. Soc.* **2016**, *97*, 1885−1908.
(35) Martin, S. T.; Artaxo, P.; Machado, L. A. T.; Manzi, A. O.; Souza, R. A. F.; Schumacher, C.; Wang, J.; Andreae, M. O.; Barbosa, H. M. J.; Fan, J.; Fisch, G.; Goldstein, A. H.; Guenther, A.; Jimenez, J. L.; Pöschl, U.; Silva Dias, M. A.; Smith, J. N.; Wendisch, M. Introduction: Observations and Modeling of the Green Ocean Amazon (GoAmazon2014/5). *Atmos. Chem. Phys.* **2016**, *16*, 4785−4797.
(36) Shilling, J. E.; Pekour, M. S.; Fortner, E. C.; Artaxo, P.; de Sá, S.; Hubbe, J. M.; Longo, K. M.; Machado, L. A. T.; Martin, S. T.; Springston, S. R.; Tomlinson, J.; Wang, J. Aircraft observations of the chemical composition and aging of aerosol in the Manaus urban plume during GoAmazon 2014/5. *Atmos. Chem. Phys.* **2018**, *18*, 10773−10797.
(37) Koop, T.; Bookhold, J.; Shiraiwa, M.; Pöschl, U. Glass transition and phase state of organic compounds: dependency on molecular properties and implications for secondary organic aerosols in the atmosphere. *Phys. Chem. Chem. Phys.* **2011**, *13*, 19238−19255.
(38) Shiraiwa, M.; Li, Y.; Tsimpidi, A. P.; Karydis, V. A.; Berkemeier, T.; Pandis, S. N.; Lelieveld, J.; Koop, T.; Pöschl, U. Global distribution of particle phase state in atmospheric secondary organic aerosols. *Nat. Commun.* **2017**, *8*, 15002.
(39) Kidd, C.; Perraud, V.; Wingen, L. M.; Finlayson Pitts, B. J. Integrating phase and composition of secondary organic aerosol from the ozonolysis of α pinene. *Proc. Natl. Acad. Sci. U.S.A.* **2014**, *111*, 7552−7557.
(40) Petters, S. S.; Kreidenweis, S. M.; Grieshop, A. P.; Ziemann, P. J.; Petters, M. D. Temperature and Humidity Dependent Phase States of Secondary Organic Aerosols. *Geophys. Res. Lett.* **2019**, *46*, 1005−1013.
(41) Renbaum Wolff, L.; Grayson, J. W.; Bateman, A. P.; Kuwata, M.; Sellier, M.; Murray, B. J.; Shilling, J. E.; Martin, S. T.; Bertram, A. K. Viscosity of α pinene secondary organic material and implications for particle growth and reactivity. *Proc. Natl. Acad. Sci. U.S.A.* **2013**, *110*, 8014−8019.
(42) Järvinen, E.; Ignatius, K.; Nichman, L.; Kristensen, T. B.; Fuchs, C.; Hoyle, C. R.; Höppel, N.; Corbin, J. C.; Craven, J.; Duplissy, J.; Ehrhart, S.; El Haddad, I.; Frege, C.; Gordon, H.; Jokinen, T.; Kallinger, P.; Kirkby, J.; Kiselev, A.; Naumann, K. H.; Petäjä, T.; Pinterich, T.; Prevot, A. S. H.; Saathoff, H.; Schiebel, T.; Sengupta, K.; Simon, M.; Slowik, J. G.; Tröstl, J.; Virtanen, A.; Vochezer, P.; Vogt, S.; Wagner, A. C.; Wagner, R.; Williamson, C.; Winkler, P. M.; Yan, C.; Baltensperger, U.; Donahue, N. M.; Flagan, R. C.; Gallagher, M.; Hansel, A.; Kulmala, M.; Stratmann, F.; Worsnop, D. R.; Möhler, O.; Leisner, T.; Schnaiter, M. Observation of viscosity transition in α pinene secondary organic aerosol. *Atmos. Chem. Phys.* **2016**, *16*, 4423−4438.
(43) Zhang, Y.; Nichman, L.; Spencer, P.; Jung, J. I.; Lee, A.; Heffernan, B. K.; Gold, A.; Zhang, Z.; Chen, Y.; Canagaratna, M. R.; Jayne, J. T.; Worsnop, D. R.; Onasch, T. B.; Surratt, J. D.; Chandler, D.; Davidovits, P.; Kolb, C. E. The Cooling Rate and Volatility Dependent Glass Forming Properties of Organic Aerosols Measured by Broadband Dielectric Spectroscopy. *Environ. Sci. Technol.* **2019**, *53*, 12366−12378.
(44) Zaveri, R. A.; Easter, R. C.; Peters, L. K. A computationally efficient Multicomponent Equilibrium Solver for Aerosols (MESA). *J. Geophys. Res.: Atmos.* **2005**, *110*, D24203.
(45) Tiedtke, M. A COMPREHENSIVE MASS FLUX SCHEME FOR CUMULUS PARAMETERIZATION IN LARGE SCALE MODELS. *Mon. Weather Rev.* **1989**, *117*, 1779−1800.
(46) Isaacman VanWertz, G.; Yee, L. D.; Kreisberg, N. M.; Wernis, R.; Moss, J. A.; Hering, S. V.; de Sá, S. S.; Martin, S. T.; Alexander, M. L.; Palm, B. B.; Hu, W.; Campuzano Jost, P.; Day, D. A.; Jimenez, J. L.; Riva, M.; Surratt, J. D.; Viegas, J.; Manzi, A.; Edgerton, E.; Baumann, K.; Souza, R.; Artaxo, P.; Goldstein, A. H. Ambient Gas Particle Partitioning of Tracers for Biogenic Oxidation. *Environ. Sci. Technol.* **2016**, *50*, 9952−9962.
(47) Nguyen, T. B.; Crounse, J. D.; Teng, A. P.; St. Clair, J. M.; Paulot, F.; Wolfe, G. M.; Wennberg, P. O. Rapid deposition of oxidized biogenic compounds to a temperate forest. *Proc. Natl. Acad. Sci. U.S.A.* **2015**, *112*, E392−E401.